Lys and Arg. However it is not so simple. Recent data suggest that FGF-2 binds not only heparin but also polysialic acid, possibly in different ways [61]. It is known that sulfation can modulate the conformation and dynamics of glycosaminoglycans, and such changes should closely correlate with different modes of binding to proteins. Deciphering how such a modification and the resulting changes in the dynamic properties regulate function is an important goal in the field of structural glycobiology.

Figure 6. Structural analysis of anti-polysialic acid antibody and oligosialic acid. (**a**) Schematic representation of a single-chain variable fragment of mAb735 (scFv735) in complex with octasialic acid is shown in the upper panel (PDB code 3WBD) [52]. Two proteins and one carbohydrate in the asymmetric unit are shown in the surface and sphere models, respectively (lower panel); (**b**) Close-up view of the carbohydrate-recognition site. Direct and water-mediated interactions between scFv735 and trisialic acid are shown in the left and right panels, respectively. Hydrogen bonds are shown as red dotted lines. Water molecules that bridge scFv735 and trisialic acid are shown as red spheres.

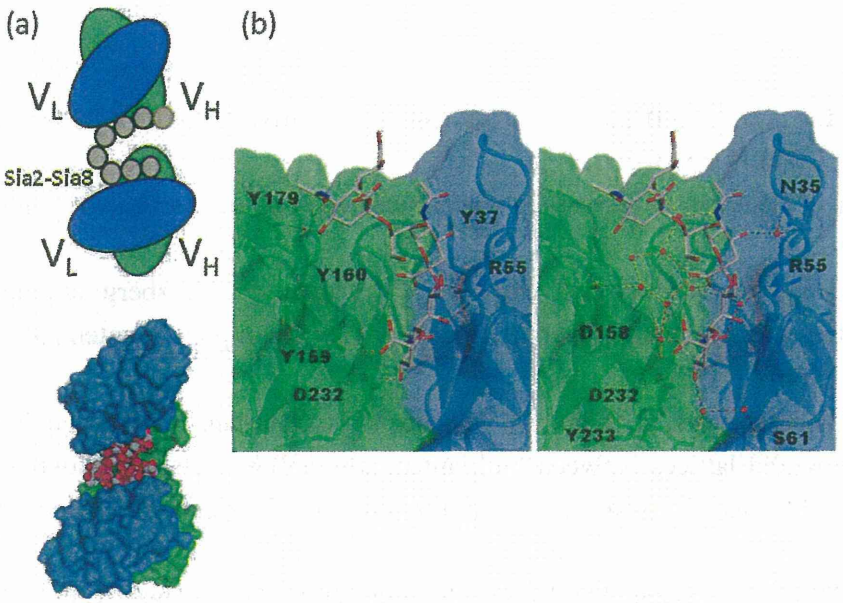

7. Conclusions and Perspectives

Carbohydrate recognition by proteins is a fundamental biological phenomenon. Data is currently accumulating on the three-dimensional structure of polysaccharide-binding proteins, showing how the proteins bind to the carbohydrate ligands. X-ray crystallography and nuclear magnetic resonance (NMR) spectroscopy are the techniques of choice in determining protein oligosaccharide interactions. X-ray data provide a static view at the atomic level. In contrast, solution NMR provides information on structure and dynamics of small to medium-sized biological molecules. X-ray and solution NMR data are complementary, and a structure determined by one technique has greater import when supported by that of the other. X-ray data derives from a stable or one of the most stable conformations of the biomolecule, but it should be noted that crystal packing can induce an unstable conformation or an artificial interaction not observed in solution. However, there are very few studies to date on oligosaccharide–protein complexes analyzed by solution NMR.

It will be also important to determine the conformation of oligosaccharides in the absence of the cognate binding protein to ascertain the effect of binding. While NMR is suitable to obtain information on conformation in solution, multiple conformations can make analysis difficult and NMR parameters, such as NOE or scalar coupling constants, are typically insufficient to determine the structure. Experimental NMR analysis and molecular dynamics simulation together can provide a truer picture of the structure and dynamics of oligosaccharides in solution.

Acknowledgments

We thank Noriko Tanaka for secretarial assistance and Masaki Kato and Mayumi Kanagawa for their helpful discussions.

Conflicts of Interest

The authors declare no conflict of interest.

References

1. Lee, R.T.; Lee, Y.C. Affinity enhancement by multivalent lectin-carbohydrate interaction. *Glycoconj. J.* **2000**, *17*, 543–551.
2. Fred Brewer, C. Binding and cross-linking properties of galectins. *Biochim. Biophys. Acta* **2002**, *1572*, 255–262.
3. Bourne, Y.; Bolgiano, B.; Liao, D.I.; Strecker, G.; Cantau, P.; Herzberg, O.; Feizi, T.; Cambillau, C. Crosslinking of mammalian lectin (galectin-1) by complex biantennary saccharides. *Nat. Struct. Biol.* **1994**, *1*, 863–870.
4. Gupta, D.; Bhattacharyya, L.; Fant, J.; Macaluso, F.; Sabesan, S.; Brewer, C.F. Observation of unique cross-linked lattices between multiantennary carbohydrates and soybean lectin. Presence of pseudo-2-fold axes of symmetry in complex type carbohydrates. *Biochemistry* **1994**, *33*, 7495–7504.
5. Olsen, L.R.; Dessen, A.; Gupta, D.; Sabesan, S.; Sacchettini, J.C.; Brewer, C.F. X-ray crystallographic studies of unique cross-linked lattices between four isomeric biantennary oligosaccharides and soybean agglutinin. *Biochemistry* **1997**, *36*, 15073–15080.
6. Rabinovich, G.A.; Toscano, M.A.; Jackson, S.S.; Vasta, G.R. Functions of cell surface galectin–glycoprotein lattices. *Curr. Opin. Struct. Biol.* **2007**, *17*, 513–520.
7. Georgelis, N.; Yennawar, N.H.; Cosgrove, D.J. Structural basis for entropy-driven cellulose binding by a type-A cellulose-binding module (CBM) and bacterial expansin. *Proc. Natl. Acad. Sci. USA* **2012**, *109*, 14830–14835.
8. Boraston, A.B.; Bolam, D.N.; Gilbert, H.J.; Davies, G.J. Carbohydrate-binding modules: Fine-tuning polysaccharide recognition. *Biochem. J.* **2004**, *382*, 769–781.
9. Boraston, A.B. The interaction of carbohydrate-binding modules with insoluble non-crystalline cellulose is enthalpically driven. *Biochem. J.* **2005**, *385*, 479–484.

10. Houston, D.R.; Recklies, A.D.; Krupa, J.C.; van Aalten, D.M. Structure and ligand-induced conformational change of the 39-kDa glycoprotein from human articular chondrocytes. *J. Biol. Chem.* **2003**, *278*, 30206–30212.
11. Fusetti, F.; Pijning, T.; Kalk, K.H.; Bos, E.; Dijkstra, B.W. Crystal structure and carbohydrate-binding properties of the human cartilage glycoprotein-39. *J. Biol. Chem.* **2003**, *278*, 37753–37760.
12. Schimpl, M.; Rush, C.L.; Betou, M.; Eggleston, I.M.; Recklies, A.D.; van Aalten, D.M. Human YKL-39 is a pseudo-chitinase with retained chitooligosaccharide-binding properties. *Biochem. J.* **2012**, *446*, 149–157.
13. Atrih, A.; Richardson, J.M.; Prescott, A.R.; Ferguson, M.A. *Trypanosoma brucei* glycoproteins contain novel giant poly-*N*-acetyllactosamine carbohydrate chains. *J. Biol. Chem.* **2005**, *280*, 865–871.
14. Barondes, S.H.; Cooper, D.N.; Gitt, M.A.; Leffler, H. Galectins. Structure and function of a large family of animal lectins. *J. Biol. Chem.* **1994**, *269*, 20807–20810.
15. Hirabayashi, J.; Hashidate, T.; Arata, Y.; Nishi, N.; Nakamura, T.; Hirashima, M.; Urashima, T.; Oka, T.; Futai, M.; Muller, W.E.; *et al.* Oligosaccharide specificity of galectins: A search by frontal affinity chromatography. *Biochim. Biophys. Acta* **2002**, *1572*, 232–254.
16. Nagae, M.; Nishi, N.; Murata, T.; Usui, T.; Nakamura, T.; Wakatsuki, S.; Kato, R. Structural analysis of the recognition mechanism of poly-*N*-acetyllactosamine by the human galectin-9 *N*-terminal carbohydrate recognition domain. *Glycobiology* **2009**, *19*, 112–117.
17. Seetharaman, J.; Kanigsberg, A.; Slaaby, R.; Leffler, H.; Barondes, S.H.; Rini, J.M. X-ray crystal structure of the human galectin-3 carbohydrate recognition domain at 2.1-Å resolution. *J. Biol. Chem.* **1998**, *273*, 13047–13052.
18. Leonidas, D.D.; Vatzaki, E.H.; Vorum, H.; Celis, J.E.; Madsen, P.; Acharya, K.R. Structural basis for the recognition of carbohydrates by human galectin-7. *Biochemistry* **1998**, *37*, 13930–13940.
19. Kumar, S.; Frank, M.; Schwartz-Albiez, R. Understanding the specificity of human Galectin-8C domain interactions with its glycan ligands based on molecular dynamics simulations. *PLoS One* **2013**, *8*, e59761.
20. Yoshida, H.; Yamashita, S.; Teraoka, M.; Itoh, A.; Nakakita, S.; Nishi, N.; Kamitori, S. X-ray structure of a protease-resistant mutant form of human galectin-8 with two carbohydrate recognition domains. *FEBS J.* **2012**, *279*, 3937–3951.
21. Stowell, S.R.; Dias-Baruffi, M.; Penttilä, L.; Renkonen, O.; Nyame, A.K.; Cummings, R.D. Human galectin-1 recognition of poly-*N*-acetyllactosamine and chimeric polysaccharides. *Glycobiology* **2004**, *14*, 157–167.
22. Di Virgilio, S.; Glushka, J.; Moremen, K.; Pierce, M. Enzymatic synthesis of natural and ^{13}C enriched linear poly-*N*-acetyllactosamines as ligands for galectin-1. *Glycobiology* **1999**, *9*, 353–364.
23. Stannard, K.A.; Collins, P.M.; Ito, K.; Sullivan, E.M.; Scott, S.A.; Gabutero, E.; Darren Grice, I.; Low, P.; Nilsson, U.J.; Leffler, H.; *et al.* Galectin inhibitory disaccharides promote tumour immunity in a breast cancer model. *Cancer Lett.* **2010**, *299*, 95–110.
24. Day, A.J.; Sheehan, J.K. Hyaluronan: Polysaccharide chaos to protein organisation. *Curr. Opin. Struct. Biol.* **2001**, *11*, 617–622.

25. Day, A.J.; Prestwich, G.D. Hyaluronan-binding proteins: Tying up the giant. *J. Biol. Chem.* **2002**, *277*, 4585–4588.
26. Day, A.J. The structure and regulation of hyaluronan-binding proteins. *Biochem. Soc. Trans.* **1999**, *27*, 115–121.
27. Goodison, S.; Urquidi, V.; Tarin, D. CD44 cell adhesion molecules. *Mol. Pathol.* **1999**, *52*, 189–196.
28. Takeda, M.; Terasawa, H.; Sakakura, M.; Yamaguchi, Y.; Kajiwara, M.; Kawashima, H.; Miyasaka, M.; Shimada, I. Hyaluronan recognition mode of CD44 revealed by cross-saturation and chemical shift perturbation experiments. *J. Biol. Chem.* **2003**, *278*, 43550–43555.
29. Teriete, P.; Banerji, S.; Noble, M.; Blundell, C.D.; Wright, A.J.; Pickford, A.R.; Lowe, E.; Mahoney, D.J.; Tammi, M.I.; Kahmann, J.D.; *et al.* Structure of the regulatory hyaluronan binding domain in the inflammatory leukocyte homing receptor CD44. *Mol. Cell* **2004**, *13*, 483–496.
30. Takeda, M.; Ogino, S.; Umemoto, R.; Sakakura, M.; Kajiwara, M.; Sugahara, K.N.; Hayasaka, H.; Miyasaka, M.; Terasawa, H.; Shimada, I. Ligand-induced structural changes of the CD44 hyaluronan-binding domain revealed by NMR. *J. Biol. Chem.* **2006**, *281*, 40089–40095.
31. Banerji, S.; Wright, A.J.; Noble, M.; Mahoney, D.J.; Campbell, I.D.; Day, A.J.; Jackson, D.G. Structures of the CD44–hyaluronan complex provide insight into a fundamental carbohydrate–protein interaction. *Nat. Struct. Mol. Biol.* **2007**, *14*, 234–239.
32. Ogino, S.; Nishida, N.; Umemoto, R.; Suzuki, M.; Takeda, M.; Terasawa, H.; Kitayama, J.; Matsumoto, M.; Hayasaka, H.; Miyasaka, M.; *et al.* Two-state conformations in the hyaluronan-binding domain regulate CD44 adhesiveness under flow condition. *Structure* **2010**, *18*, 649–656.
33. Lesley, J.; Hascall, V.C.; Tammi, M.; Hyman, R. Hyaluronan binding by cell surface CD44. *J. Biol. Chem.* **2000**, *275*, 26967–26975.
34. Lesley, J.; Gál, I.; Mahoney, D.J.; Cordell, M.R.; Rugg, M.S.; Hyman, R.; Day, A.J.; Mikecz, K. TSG-6 modulates the interaction between hyaluronan and cell surface CD44. *J. Biol. Chem.* **2004**, *279*, 25745–25754.
35. Blundell, C.D.; Mahoney, D.J.; Almond, A.; DeAngelis, P.L.; Kahmann, J.D.; Teriete, P.; Pickford, A.R.; Campbell, I.D.; Day, A.J. The link module from ovulation- and inflammation-associated protein TSG-6 changes conformation on hyaluronan binding. *J. Biol. Chem.* **2003**, *278*, 49261–49270.
36. Chuah, C.T.; Sarko, A.; Deslandes, Y.; Marchessault, R.H. Packing analysis of carbohydrates and polysaccharides.14. Triple-helical crystalline-structure of curdlan and paramylon hydrates. *Macromolecules* **1983**, *16*, 1375–1382.
37. Sletmoen, M.; Stokke, B.T. Higher order structure of (1,3)-b-D-glucans and its influence on their biological activities and complexation abilities. *Biopolymers* **2008**, *89*, 310–321.
38. Saito, H.; Yoshioka, Y.; Uehara, N.; Aketagawa, J.; Tanaka, S.; Shibata, Y. Relationship between conformation and biological response for (1→3)-β-D-glucans in the activation of coagulation factor G from limulus amebocyte lysate and host-mediated antitumor activity. Demonstration of single-helix conformation as a stimulant. *Carbohydr. Res.* **1991**, *217*, 181–190.
39. Boraston, A.B.; Nurizzo, D.; Notenboom, V.; Ducros, V.; Rose, D.R.; Kilburn, D.G.; Davies, G.J. Differential oligosaccharide recognition by evolutionarily-related β-1,4 and β-1,3 glucan-binding modules. *J. Mol. Biol.* **2002**, *319*, 1143–1156.

40. Van Bueren, A.L.; Morland, C.; Gilbert, H.J.; Boraston, A.B. Family 6 carbohydrate binding modules recognize the non-reducing end of β-1,3-linked glucans by presenting a unique ligand binding surface. *J. Biol. Chem.* **2005**, *280*, 530–537.
41. Hoffmann, J.A. The immune response of *Drosophila*. *Nature* **2003**, *426*, 33–38.
42. Takahasi, K.; Ochiai, M.; Horiuchi, M.; Kumeta, H.; Ogura, K.; Ashida, M.; Inagaki, F. Solution structure of the silkworm βGRP/GNBP3 *N*-terminal domain reveals the mechanism for β-1,3-glucan-specific recognition. *Proc. Natl. Acad. Sci. USA* **2009**, *106*, 11679–11684.
43. Kanagawa, M.; Satoh, T.; Ikeda, A.; Adachi, Y.; Ohno, N.; Yamaguchi, Y. Structural insights into recognition of triple-helical β-glucans by an insect fungal receptor. *J. Biol. Chem.* **2011**, *286*, 29158–29165.
44. Dai, H.; Hiromasa, Y.; Takahashi, D.; VanderVelde, D.; Fabrick, J.A.; Kanost, M.R.; Krishnamoorthi, R. An initial event in the insect innate immune response: Structural and biological studies of interactions between β-1,3-glucan and the *N*-terminal domain of β-1,3-glucan recognition protein. *Biochemistry* **2013**, *52*, 161–170.
45. Palma, A.S.; Feizi, T.; Zhang, Y.; Stoll, M.S.; Lawson, A.M.; Díaz-Rodríguez, E.; Campanero-Rhodes, M.A.; Costa, J.; Gordon, S.; Brown, G.D.; *et al.* Ligands for the β-glucan receptor, Dectin-1, assigned using "designer" microarrays of oligosaccharide probes (neoglycolipids) generated from glucan polysaccharides. *J. Biol. Chem.* **2006**, *281*, 5771–5779.
46. Hanashima, S.; Ikeda, A.; Tanaka, H.; Adachi, Y.; Ohno, N.; Takahashi, T.; Yamaguchi, Y. NMR study of short β(1–3)-glucans provides insights into the structure and interaction with Dectin-1. *Glycoconj. J.* **2013**, doi:10.1007/s10719-013-9510-x.
47. Meagher, J.L.; Winter, H.C.; Ezell, P.; Goldstein, I.J.; Stuckey, J.A. Crystal structure of banana lectin reveals a novel second sugar binding site. *Glycobiology* **2005**, *15*, 1033–1042.
48. Nakata, D.; Troy, F.A., 2nd. Degree of polymerization (DP) of polysialic acid (polySia) on neural cell adhesion molecules (N-CAMS): Development and application of a new strategy to accurately determine the DP of polySia chains on N-CAMS. *J. Biol. Chem.* **2005**, *280*, 38305–38316.
49. Sato, C.; Kitajima, K. Disialic, oligosialic and polysialic acids: Distribution, functions and related disease. *J. Biochem.* **2013**, *154*, 115–136.
50. Finne, J. Occurrence of unique polysialosyl carbohydrate units in glycoproteins of developing brain. *J. Biol. Chem.* **1982**, *257*, 11966–11970.
51. Hanashima, S.; Sato, C.; Tanaka, H.; Takahashi, T.; Kitajima, K.; Yamaguchi, Y. NMR study into the mechanism of recognition of the degree of polymerization by oligo/polysialic acid antibodies. *Bioorg. Med. Chem.* **2013**, *21*, 6069–6076.
52. Nagae, M.; Ikeda, A.; Hane, M.; Hanashima, S.; Kitajima, K.; Sato, C.; Yamaguchi, Y. Crystal structure of anti-polysialic acid antibody single chain Fv fragment complexed with octasialic acid: Insight into the binding preference for polysialic acid. *J. Biol. Chem.* **2013**, *288*, 33784–33796.
53. Evans, S.V.; Sigurskjold, B.W.; Jennings, H.J.; Brisson, J.R.; To, R.; Tse, W.C.; Altman, E.; Frosch, M.; Weisgerber, C.; Kratzin, H.D.; *et al.* Evidence for the extended helical nature of polysaccharide epitopes. The 2.8 Å resolution structure and thermodynamics of ligand binding of an antigen binding fragment specific for α-(2→8)-polysialic acid. *Biochemistry* **1995**, *34*, 6737–6744.

54. Yamasaki, R.; Bacon, B. Three-dimensional structural analysis of the group B polysaccharide of *Neisseria meningitidis* 6275 by two-dimensional NMR: The polysaccharide is suggested to exist in helical conformations in solution. *Biochemistry* **1991**, *30*, 851–857.
55. Brisson, J.R.; Baumann, H.; Imberty, A.; Pérez, S.; Jennings, H.J. Helical epitope of the group B meningococcal α(2–8)-linked sialic acid polysaccharide. *Biochemistry* **1992**, *31*, 4996–5004.
56. Yongye, A.B.; Gonzalez-Outeiriño, J.; Glushka, J.; Schultheis, V.; Woods, R.J. The conformational properties of methyl α-(2,8)-di/trisialosides and their *N*-acyl analogues: Implications for anti-*Neisseria meningitidis* B vaccine design. *Biochemistry* **2008**, *47*, 12493–12514.
57. Henderson, T.J.; Venable, R.M.; Egan, W. Conformational flexibility of the group B meningococcal polysaccharide in solution. *J. Am. Chem. Soc.* **2003**, *125*, 2930–2939.
58. Jin, L.; Abrahams, J.P.; Skinner, R.; Petitou, M.; Pike, R.N.; Carrell, R.W. The anticoagulant activation of antithrombin by heparin. *Proc. Natl. Acad. Sci. USA* **1997**, *94*, 14683–14688.
59. Faham, S.; Hileman, R.E.; Fromm, J.R.; Linhardt, R.J.; Rees, D.C. Heparin structure and interactions with basic fibroblast growth factor. *Science* **1996**, *271*, 1116–1120.
60. Capila, I.; Hernáiz, M.J.; Mo, Y.D.; Mealy, T.R.; Campos, B.; Dedman, J.R.; Linhardt, R.J.; Seaton, B.A. Annexin V–heparin oligosaccharide complex suggests heparan sulfate-mediated assembly on cell surfaces. *Structure* **2001**, *9*, 57–64.
61. Ono, S.; Hane, M.; Kitajima, K.; Sato, C. Novel regulation of fibroblast growth factor 2 (FGF2)-mediated cell growth by polysialic acid. *J. Biol. Chem.* **2012**, *287*, 3710–3722.

Bioorganic & Medicinal Chemistry 21 (2013) 6069–6076

Contents lists available at ScienceDirect

Bioorganic & Medicinal Chemistry

journal homepage: www.elsevier.com/locate/bmc

NMR study into the mechanism of recognition of the degree of polymerization by oligo/polysialic acid antibodies

Shinya Hanashima [a,*], Chihiro Sato [b], Hiroshi Tanaka [c], Takashi Takahashi [c], Ken Kitajima [b], Yoshiki Yamaguchi [a,*]

[a] Structural Glycobiology Team, RIKEN ASI, Saitama 351-0198, Japan
[b] Graduate School of Bioagricultural Sciences and Bioscience and Biotechnology Center, Nagoya University, Nagoya 464-8601, Japan
[c] Graduate School of Science and Engineering, Tokyo Institute of Technology, Meguro, Tokyo 152-8552, Japan

ARTICLE INFO

Article history:
Received 27 March 2013
Revised 9 July 2013
Accepted 10 July 2013
Available online 29 July 2013

Keywords:
Polysialic acid
Conformation
Antibody
STD-NMR
TR-NOE

ABSTRACT

Oligo/polysialic acids consisting of consecutive α(2,8)-linkages on gangliosides and glycoproteins play a role in cell adhesion and differentiation events in a manner that is dependent on the degree of polymerization (DP). Anti-oligo/polysialic acid antibodies often have DP-dependent antigenic specificity, and such unique antibodies are often used in biological studies for the detection and differentiation of oligo/polysialic acids. However, molecular mechanisms remain unclear. We here use NMR techniques to analyze the binding epitopes of the anti-oligo/polysialic acid monoclonal antibodies (mAb) A2B5 and 12E3. The mAb A2B5, which has a preference for trisialic acid, recognizes sialic acid residues at the non-reducing terminus and those in nascent units. On the other hand, mAb 12E3, which prefers oligo/polysialic acids of more than six sugar units, recognizes inner sialic acid residues. In both structural complexes, the interresidue transferred NOE correlations are significantly different from those arising from analogs of the free states, indicating that the bound and free sugar conformations are distinct. The ability of the two mAbs to distinguish the chain lengths comes from different binding epitopes and possibly from the conformational differences in the oligo/polysialic acids. Information on the recognition modes is needed for the structural design of immunoreactive antigens for the development of high-affinity anti-polysialic acid antibodies and of related vaccines against pathogenic, polysialic acid-coated bacteria.

1. Introduction

Oligo/polysialic acid is a homopolymer of sialic acid with the degree of polymerization (DP) ranging from 3 to >400 residues.[1,2] The homopolymers are conjugated with gangliosides and with some specific glycoproteins at the mammalian cell surface, and are especially involved in nerve cell adhesion and differentiation.[2] Oligosialic acid units are abundant at the non-reducing terminus of gangliosides. For example, the majority of disialic acids (Neu5Acα(2-8)Neu5Ac) are attached on b-series gangliosides. One of the major b-series gangliosides, GD3, is implicated in CD95-mediated and ceramide-mediated apoptosis[3] and malignant transformation of melanoma.[4] The c-series gangliosides carrying trisialic acids (Neu5Acα(2-8)Neu5Acα(2-8)Neu5Ac) occur at brain and nerve cell surfaces.[5,6]

In contrast, some of the specific glycoproteins have polysialic acids of α(2-8)Neu5Ac units. A noteworthy example is the family of carrier proteins or neuronal cell adhesion molecules (NCAMs) which play an important role in the formation of the nervous system.[7] NCAMs have at least two polysialic acid chains at their *N*-glycan termini, and their well-arranged array of negative charges has an anti-adhesive effect.[8] The polysialic acids regulate the concentrations of the brain-derived neurotrophic factor (BDNF) and fibroblast growth factor 2 (FGF2) in a DP dependent manner.[9,10] Polysialic acids also occur in tumor-associated tissues.[11] The DP of the oligo/polysialic acids correlates with particular biological functions. Recently, oligosialylated glycoproteins occurring at different stages of development have been identified in the mammalian brain.[12,13]

Oligo/polysialic acids with α(2,8), α(2,9) and α(2,8/9) linkages are also found in pathogenic bacteria including strains of *Escherichia coli* K1 and *Neisseria meningitidis*. The latter is a major cause of bacterial meningitis in developed countries.[14,15] Such bacteria escape the host immune system through a hydration effect of the highly hydrophilic encapsulated polysialic acids and a repulsion effect due to net negative charges.[16] Even so, antibodies against polysialic acid with α(2-8)-linkage are found following infection with serogroup B *Neisseria meningitidis*.[17] The antibodies recognize more than 10 sialic acid units,[18] leading to a conformational epitope hypothesis,[19] in which a particular conformation, believed to be a helix, is the targeted antigen.

A flexible helical structure was suggested by early nuclear magnetic resonance (NMR) analyses with the aid of molecular model-

* Corresponding authors.
E-mail addresses: shanashima@riken.jp (S. Hanashima), yyoshiki@riken.jp (Y. Yamaguchi).

0968-0896/$ - see front matter © 2013 Elsevier Ltd. All rights reserved.
http://dx.doi.org/10.1016/j.bmc.2013.07.023

ing and dynamics calculations.[20–23] Brisson et al. and Yamasaki et al. independently reported the helical structures based on nuclear Overhauser effect (NOE) and three-bond scholar coupling constant ($^3J_{H-H}$) of the analysis of oligosialic acid.[22,23] However, the pitches of the proposed helices have significant difference. More recently Yongye et al. reported another helical structure based on trisialic acid analysis using high-field NMR with molecular dynamic simulations.[21] One of the causes of the diversity is the small number of inter-residual NOE correlations, which fails to adequately constrain the φ and ψ angles. Recently, Battistel et al. performed an NMR structural analysis using an uniformly ^{13}C,^{15}N-labeled tetramer of α(2-8)sialic acid, and found the O8-HN5 hydrogen bond which directly constrains the ω angles.[20] In sharp contrast, an NMR relaxation analysis of spin–lattice relaxation (^{13}C T_1), transverse relaxation (^{13}C T_2) and ^{13}C–{^1H} heteronuclear NOE suggests that polysialic acid does not assume a helical structure at all but rather a random coil.[24] Although the functions of the oligo/polysialic acids on glycolipids and glycoproteins relate to their 3D structure, the actual conformation(s) remains unclear.

Monoclonal antibodies (mAbs) against oligo/polysialic acids have been investigated not only for clinical purposes but also as a powerful tool to analyze the function of polysialic acid.[18,25] To date, their DP-dependent interaction properties have been identified using biochemical techniques. However, studies which reveal details of the binding modes are few, presumably due to the poorly-separated NMR signals of repeating Neu5Ac units or the difficulty in obtaining crystals for X-ray study. One X-ray crystal structure of the Fab fragment of an anti-polysialic acid antibody mAb735 (murine IgG_{2a}) with in silico docking of a sugar chain suggests that the binding site is a shallow groove that could accept a helical polysialic acid.[26] Recently, the X-ray crystal structure of N-propionylated polysialic acid-specific antibodies was also reported.[27] The empty binding site was rationally filled with the *N*-propionyl polysialci acid by the docking study with NMR data.

Here, in order to gain insight into the mechanism of DP-dependent binding, we have determined the binding epitopes and studied the bound conformations of oligo/polysialic acids in complex with monoclonal antibodies A2B5 (IgM) and 12E3 (IgM). The former discriminates the tri-α(2,8)Neu5Ac unit from other chain-lengths,[12] and the latter has a binding preference for more than 5-successive α(2,8)Neu5Ac residues.[18] We used saturation transfer difference (STD) NMR and the antigens octyl-$(Neu5Ac)_3$ and $(Neu5Ac)_6$ (Fig. 1). The NMR method is now widely applied for the analysis of various types of binding in solution, such as protein-small molecular weight ligand screening as well as determining protein–protein interactions.[28,29] 2D ^1H–^1H NOESY was employed for the conformational analysis of the oligosialic acids in free and bound states.[30,31]

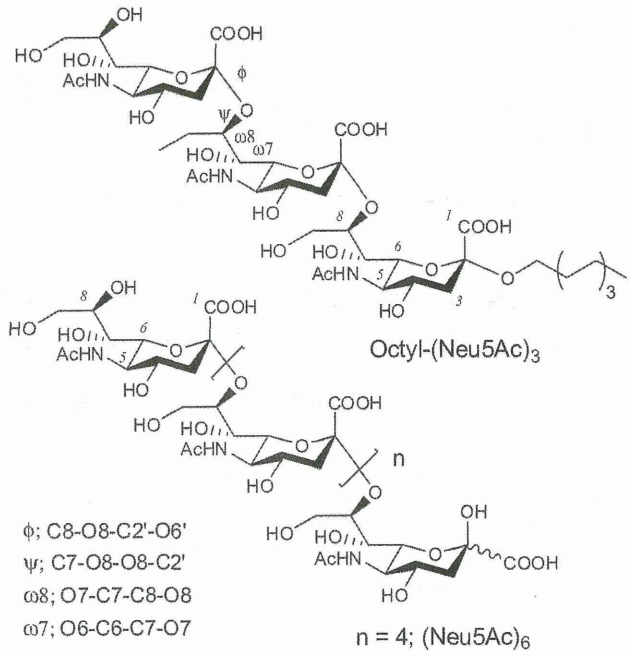

Figure 1. Structures of oligosialic acids. Octyl-$(Neu5Ac)_3$ and $(Neu5Ac)_6$ were used for STD-NMR analysis.

2. Results

2.1. Binding analysis of octyl-$(Neu5Ac)_3$ with mAb A2B5

NMR-based binding experiments between octyl-$(Neu5Ac)_3$ and mAb A2B5 were first performed by titrating antigen into the antibody solution (10 μM/binding site) from 0.5 to 10 molar equivalents. The ligand signal showed significant broadening due to binding to the large molecular-weight protein (Fig. S1).

STD-NMR experiments were then performed to determine the binding epitopes (Fig. 2). Upon screening of the optimum STD-NMR conditions, the experimental temperature was set at 10 °C (Figs. S5 and S6). Furthermore, direct and water-mediated saturation artifacts were not observed under the conditions using D_2O solvent system (Fig. S7). 1D STD-NMR provides the characteristic binding pattern (spectrum B) in the comparison to ^1H NMR (spectrum A). Reporter signals are located at an isolated singlet of acetyls (2.0–2.2 ppm) originating from N-acetamide groups at C-5, as well as at C-3 equatorial protons (2.6–2.9 ppm). Remarkably, the sharp acetyl signal of residue (c) at 2.07 ppm shows a higher saturation transfer effect than the other two acetyl signals. These observations indicate that mAb A2B5 interacts most strongly around the C-5 N-acetamide moiety of the non-reducing terminus (c)-unit. In contrast to the N-acetamide, the protons at C-5 and C-3 show little relative-intensity changes, suggesting that they are not part of the direct binding interface.

Although 1D ^1H-STD-NMR is sensitive enough to identify binding between proteins and their ligands, serious signal overlapping prevents further spectral analysis at atomic level resolution. To overcome this, we performed 2D ^1H–^{13}C STD-HSQC experiments. An overlay of ^1H–^{13}C HSQC spectra clearly indicated that the addition of mAb A2B5 provided only a limited signal changes for octyl-$(Neu5Ac)_3$ (Fig. 3A). An overlay of ^1H–^{13}C HSQC and STD-HSQC spectra focusing on the pyranose ring (C4–C6) and side-chain (C7–C9) signals are shown in Figure 3B. The overlay of STD-HSQC spectra to the protons attached at C5, C6, C7 and C8 showed stronger STD signals (red) than those at other positions.

The binding epitope of octyl-$(Neu5Ac)_3$ on mAb A2B5 is summarized in Figure 4. The relative values (%) were standardized using the STD amplification factor (AF) with a maximum value of AF at an Ac group taken as 100%. The distribution of higher relative values occurs especially at the non-reducing terminus residue (c) and the middle residue (b) rather than at the residue at the reducing end (a). A remarkably high value was assigned to the N-acetamide group of residue (c). The observation is consistent with the 1D-STD data which also indicated strongest saturation transfer effect with the reporter N-acetamide residue. The protons at C4, C6 and C7 on residue b and c have relatively higher values than those at C3, C5 and C8. The evidence suggests that mAb A2B5 preferentially binds the α-face of the pyranose ring at residues (b) and (c).

Then, 2D ^1H–^1H NOESY was performed to analyze whether the bound trisialic acid assumes a particular conformation, distinct from the free form (Fig. 5).[30] A comparison of the two NOE spectra

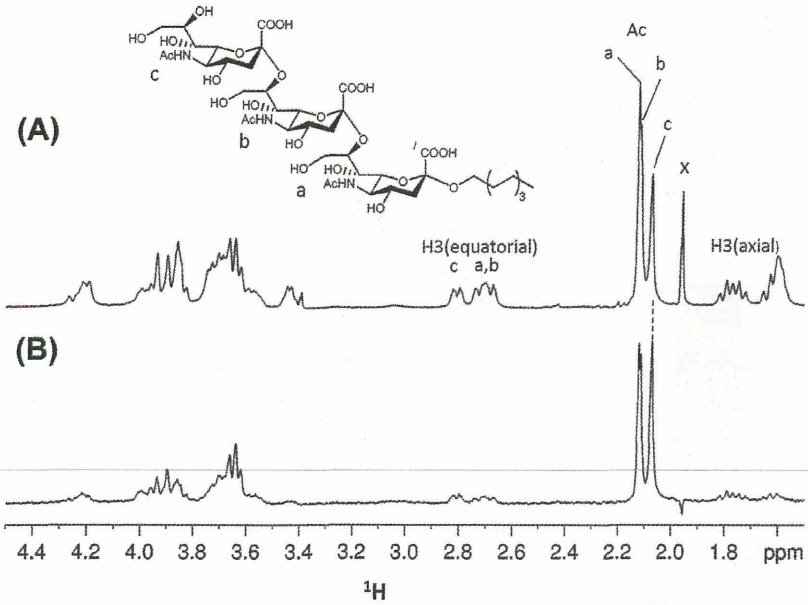

Figure 2. 1D ^{1}H NMR spectrum (A) and ^{1}H-STD-NMR spectrum (B) of 10 μM (binding site) anti-oligo/polysialic acid antibody A2B5 (IgM) with octyl-$(Neu5Ac)_3$ (50 equiv) in PBS composed with 99% D_2O (pH 7.4). Protein signal at 7 ppm was irradiated for saturation and 40 ppm was irradiated for reference. x; impurity.

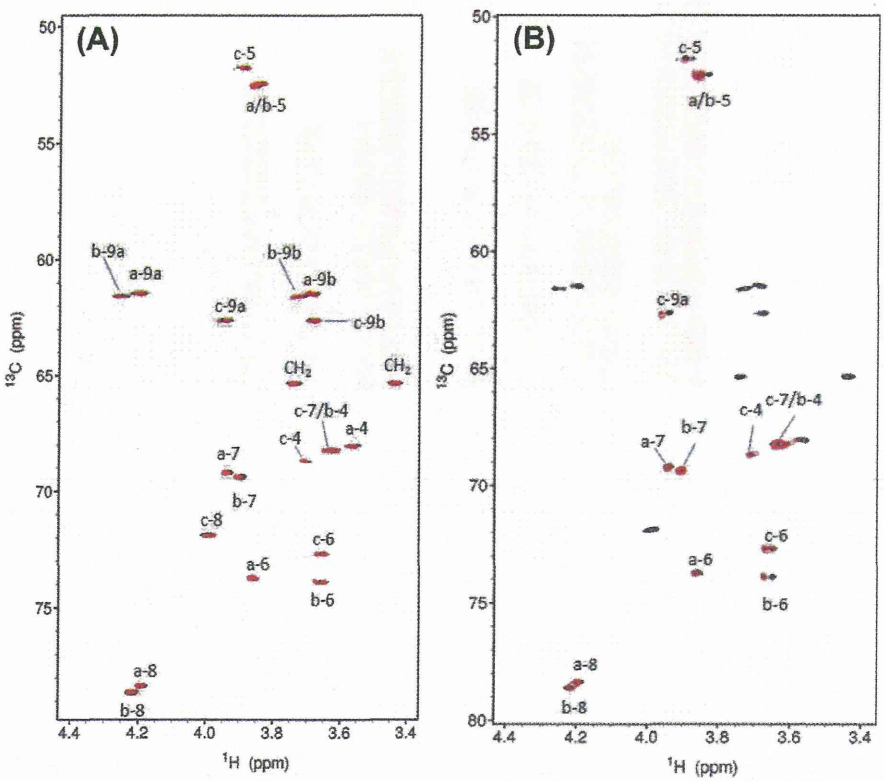

Figure 3. 2D ^{1}H–^{13}C HSQC spectra of octyl-$(Neu5Ac)_3$. (A) Overlay of 2D ^{1}H–^{13}C HSQC spectrum of octyl-$(Neu5Ac)_3$ (black) and octyl-$(Neu5Ac)_3$ (50 equiv) with 20 μM anti-oligo/polysialic acid antibody A2B5 (IgM) (red). (B) Overlay of 2D ^{1}H–^{13}C HSQC spectrum of octyl-$(Neu5Ac)_3$ (50 equiv) with 20 μM anti-oligo/polysialic acid antibody 12E3 (IgM) (black) and 2D ^{1}H–^{13}C STD-HSQC spectrum (red) in PBS with 99% D_2O. Protein signal at 7 ppm was irradiated for saturation and 40 ppm was irradiated for reference.

shows that the inter-residual NOE correlations between H3-axial of residue (b) and H8 of residue a as well as H3-axial of residue (c) and H8 of residue b are clearly diminished in the presence of mAb A2B5 (Fig. 5A and B). The distances of the protons, which were calculated from inter-residual NOE intensities of free and bound states, are summarized in Table S1. They apparently reveal rotations of the φ and/or ψ angles of glycoside bonds at residues (c-b) and (b-a) upon binding to mAb A2B5.

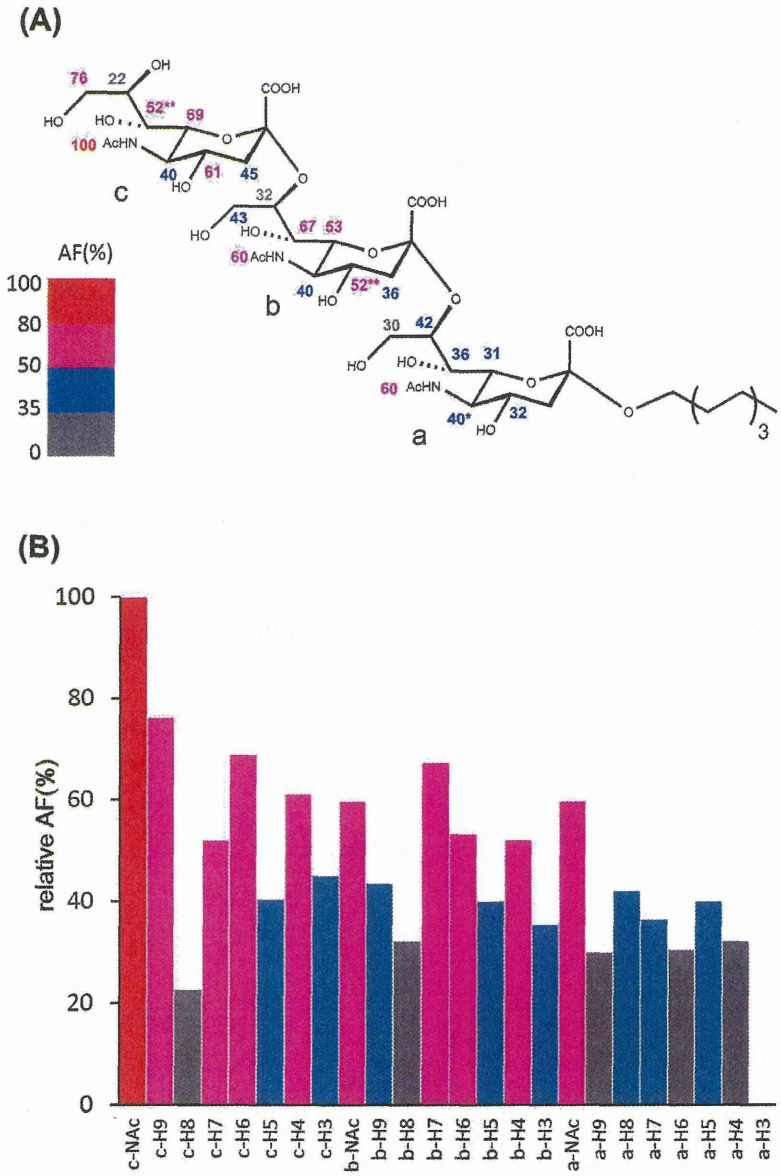

Figure 4. *Binding epitope of octyl-(Neu5Ac)$_3$ to mAb A2B5. The maximum value of AF at an Ac group was taken as 100% and the relative intensities (%) are indicated. The* AF(%) was shown on structure (A) and graph (B) with the colors of the respective AF(%)s. The relative values of the amide and C3 protons were originally determined with a 1D-STD spectrum and standardized by an Ac signal taken as the 100% value. Overlapping signals were formally assigned the same value of AF.

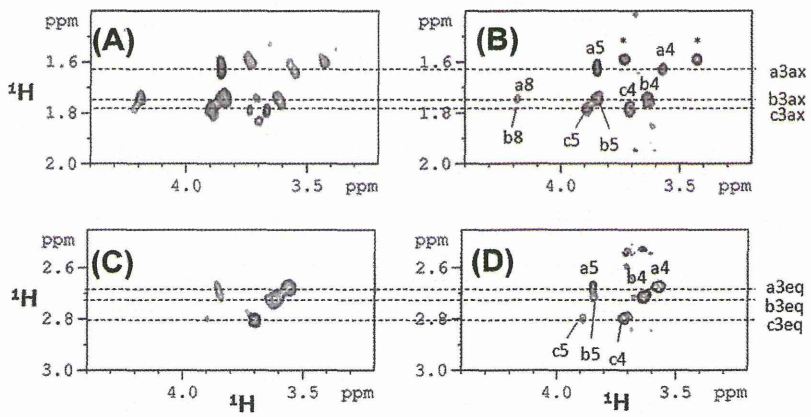

Figure 5. 2D ^{1}H–^{1}H NOESY and TR-NOESY spectra of octyl-(Neu5Ac)$_3$. (A) NOE correlations of H3-axial region of octyl-(Neu5Ac)$_3$ (1.0 mM). (B) NOE correlations of H3-axial region of octyl-(Neu5Ac)$_3$ (10 equiv) in the presence of mAb A2B5 (15 μM). (C) NOE correlations of H3-equatorial region of octyl-(Neu5Ac)$_3$. (D) NOE correlations of H3-equatorial region of octyl-(Neu5Ac)$_3$ (10 equiv) in the presence of mAb A2B5.

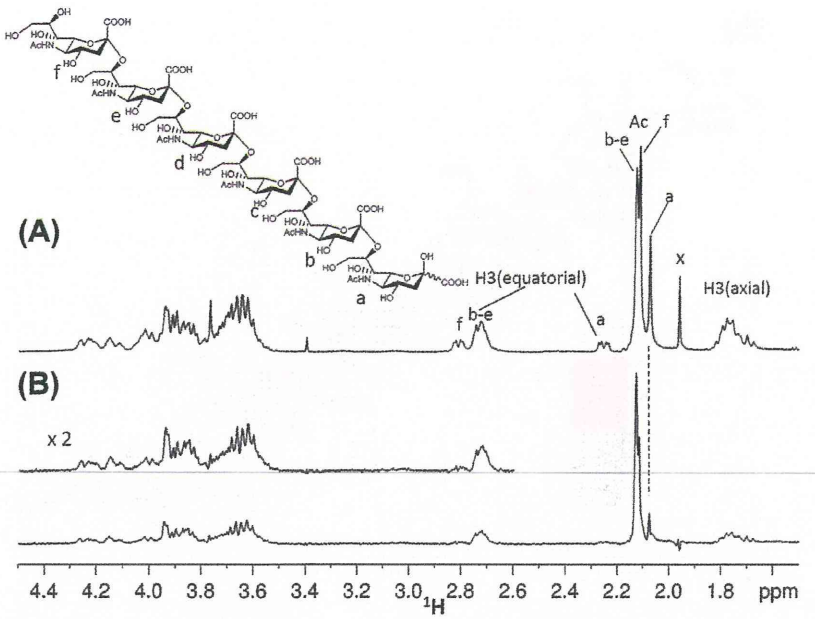

Figure 6. 1D STD-NMR spectra of 10 μM (binding site) anti-oligo/polysialic acid antibody 12E3 (IgM) with $(Neu5Ac)_6$ (50 equiv) in PBS composed with 99% D_2O (pH 7.4). ^{1}H NMR spectrum (reference spectrum irradiated at 40 ppm) (A) and 1D STD-NMR spectrum (B) are indicated. Protein signal at 7 ppm was irradiated for saturation and 40 ppm was irradiated for reference. x; impurity.

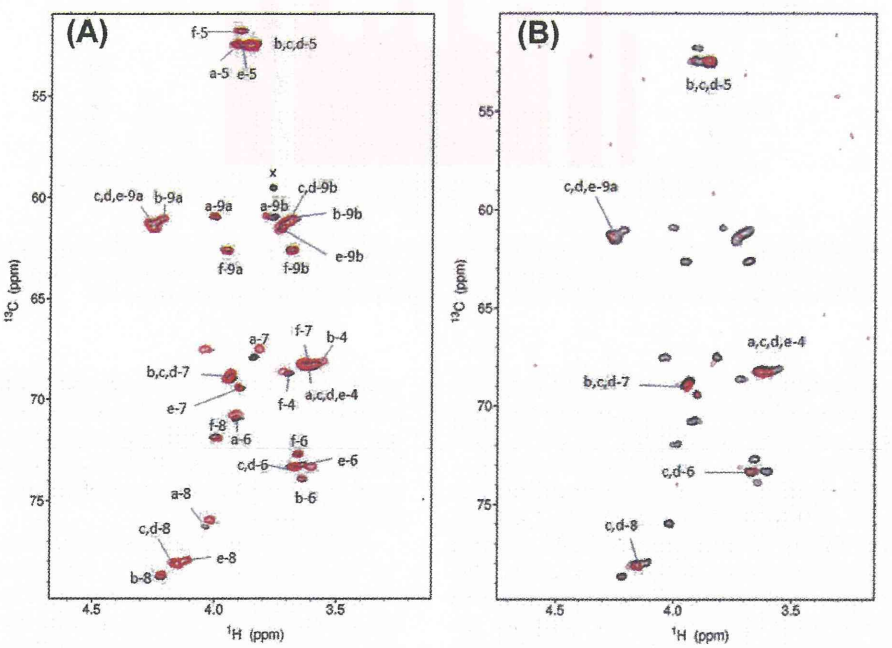

Figure 7. 2D ^{1}H–^{13}C HSQC spectra of $(Neu5Ac)_6$. (A) Overlay of 2D ^{1}H–^{13}C HSQC spectrum of $(Neu5Ac)_6$ (black) and $(Neu5Ac)_6$ (50 equiv) with 20 μM anti-oligo/polysialic acid antibody 12E3 (IgM) (red). (B) Overlay of 2D ^{1}H–^{13}C HSQC spectrum of $(Neu5Ac)_6$ (50 equiv) with 20 μM anti-oligo/polysialic acid antibody 12E3 (IgM) (black) and 2D ^{1}H–^{13}C STD-HSQC spectrum (red) in PBS with 99% D_2O. Protein signal at 7 ppm was irradiated for saturation and 40 ppm was irradiated for reference.

2.2. Binding analysis of $(Neu5Ac)_6$ with mAb 12E3

A titration experiment was performed by gradually adding $(Neu5Ac)_6$ to a solution of mAb 12E3 (10 μM/binding site) from 0 to 10 equiv (Fig. S2). The signal originating from $(Neu5Ac)_6$ is significantly broadened on binding to the antibody, especially in the molar ratio of 1–5 equiv, due to the slow tumbling of the bound fraction under the NMR time scale. In addition, there are no changes in chemical shifts under these conditions.

Further binding analysis was performed using STD-NMR for the determination of the binding epitope. As in the case of the complex of A2B5 and octyl-$(Neu5Ac)_3$, sharp acetyl signals, and C3-H signals serve as good indicators in the 1D ^{1}H-STD-NMR spectrum (Fig. 6).[32] Especially noteworthy is the remarkable augmentation of the signal

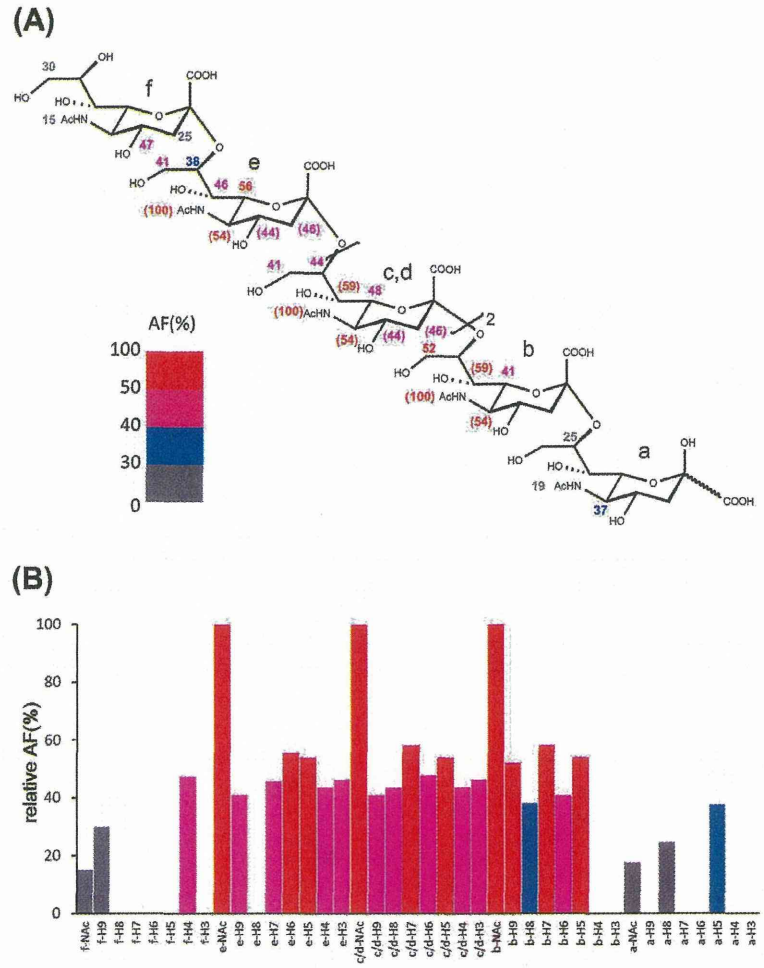

Figure 8. Binding epitope of $(Neu5Ac)_6$ complexed to mAb 12E3. The maximum value of AF at an Ac group was taken as 100% and relative intensities (%) are indicated. The AF(%) was shown on structure (A) and graph (B) with the colors of the respective AF(%)s. The relative values of the amide and C3 protons were originally determined with a 1D-STD spectrum standardized on an Ac signal taken as 100%. Overlapping signals were formally assigned the same value of AF.

intensities of the *N*-acetyl groups from the inner residues (b–e) over those from outer residues, reducing terminus (a) and non-reducing terminus (f). These consistent observations indicate that mAb 12E3 especially recognizes the inner sialic acid residues of $(Neu5Ac)_6$.

Further analysis of the binding epitope in high resolution was achieved with 2D ^1H–^{13}C STD-HSQC. An overlay of ^1H–^{13}C HSQC spectra clearly indicated that the addition of mAb 12E3 provided slight changes to the signal originating from residue a (Fig. 7A). An overlay of ^1H–^{13}C HSQC and STD-HSQC spectra focusing on the pyranose ring (C4–C6) and side-chain (C7–C9) signals are shown in Figure 7B. The HSQC spectrum resolves the set of signals originating from reducing and non-reducing terminal residues (a) and (f), but those from inner residues (c) and (d) mostly overlap. The signals from residues (b) and (e) are isolated in parts. The STD-HSQC signals arise from C4, C5, C6, C7, and C8 of inner sialic acid residues.

We used AF (Fig. 8). Overlapping signals were formally assigned the same value of AF. Higher relative AF values are distributed around inner sialic acid residues (c) and (d), followed by those around residues (b) and (e). In contrast, lower AF values are associated with the residues (a) and (f) at reducing and non-reducing termini. The analysis suggests that mAb 12E3 preferentially recognizes inner residues (c) and (d), rather than the terminal residues (a) and (f). This conclusion is consistent with the 1D-STD NMR analysis using reporter N-Ac groups, suggesting interaction at residues (b), (c), (d) and (e). The 2D STD-HSQC NMR analysis picked out inner residues as the principal contact points. Although the binding moiety within a Neu5Ac residue is comparable to that seen in the case of mAb A2B5-octyl$(Neu5Ac)_3$, the face-selective recognition pattern is absent.

Analysis of the bound conformation was performed by 2D ^1H–^1H NOESY at a ratio of 1:10 (10 μM/binding site of the 12E3:$(Neu5Ac)_6$) (Fig. 9). In comparison with the NOESY correlations of the free ligand, some signals were significantly diminished the presence of mAb 12E3. Particularly, an inter-residue NOE correlation of H3-axial of residue (f) to H8 of residue (e), shown in Figure 9A, was diminished in the presence of mAb 12E3 (Fig. 9B). Further, comparing Figure 9C with Figure 9D, the signal intensities of H3-equatorials of residues (c, d, e) to H8 of residues (b, c, d) were also diminished. All indicated protons belong to the glycoside bonds and hinge region of the oligosialic acid structure. It shows that rotation of the dihedral angles, specifically φ and ψ, are required to assume a bound conformation.

3. Discussion

We have determined the antigen binding epitopes in the complexes mAb A2B5/octyl-$(Neu5Ac)_3$ and mAb 12E3/$(Neu5Ac)_6$ by

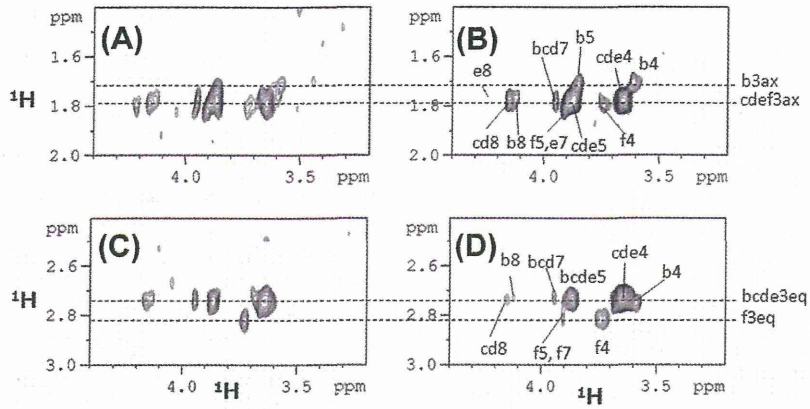

Figure 9. 2D ^{1}H–^{1}H NOESY and TR-NOESY spectra of $(Neu5Ac)_6$. (A) NOE correlations of H3-axial region of $(Neu5Ac)_6$ (1.5 mM). (B) NOE correlations of H3-axial region of $(Neu5Ac)_6$ (10 equiv) in the presence of mAb 12E3 (10 μM, binding site). (C) NOE correlations of H3-equatorial region of $(Neu5Ac)_6$. (D) NOE correlations of H3-equatorial region of $(Neu5Ac)_6$ (10 M equiv) in the presence of mAb 12E3.

NMR in an effort to account for the specificity differences of the antibodies. Apparent differences of the binding epitope were observed by STD-NMR analysis: mAb A2B5 preferentially interacts with the residue at non-reducing termini of the trisialic acid, while mAb 12E3 interacts with inner residues of hexasialic acid. The DP-dependent binding preferences of mAbs A2B5 and 12E3 are exclusive, with very limited cross reaction with confirmed by ELISA-type assay.[12,13] We consider that the difference between the epitopes is a key to understanding the DP-dependent binding preferences of the antibodies.

The DP-dependency is expected to originate from the complementarity of the bound conformations of the ligands and the shape of the binding site, which would dictate unique favorable binding interactions. STD-NMR indicates that both mAb A2B5 and 12E3 especially interact with the N-acetamide-C5-C6-C7-C8. It would reveal that both mAbs recognize corresponding conformations of α(2-8)Neu5Ac because the dihedral angles,φ, ψ, $\omega 7$, and $\omega 8$, consisting with C6-C7-C8-O8-C2′ which are closely related to the structure of α(2-8)Neu5Ac,[20–24] and are constrained by hydrogen bond between N-acetamide and O8.[20] In both complexes, the bound NOE correlations of H3axial-H8′ of octyl-$(Neu5Ac)_3$ and H3equatrial-H8′ of $(Neu5Ac)_6$ have a different patterns from the free state (Figs. 5 vs 9). It reveals that flexible solution conformations of the ligands are constrained to be a bound conformer. A model of the bound conformer of octyl-$(Neu5Ac)_3$ complexed with A2B5 was constructed based on a reported free structure together with fulfilling the TR-NOE correlations[21] (Fig. S3). The protons showing potent STD effects at the α-face of both units (b) and (c) are on the same side and form a binding face. The binding manner is compatible with the proposed recognition mechanism of mAb ME36.1 for GD2 ganglioside where the binding site is a shallow pit.[33] The similarity is reasonable because mAb A2B5 was originally developed for oligodendrocyte progenitor cells, and their innate binding ligands are reported as GT3, GT1c, GQ1c and GP1c gangliosides, all of which include the α(2-8)Neu5Ac moiety.[34,35]

A model of $(Neu5Ac)_6$ bound to 12E3 was also constructed (Fig. S4). Here TR-NOE correlations of H3equatrial-H8′ are diminished. This binding manner is analogous to a model of anti-polysialic acid antibody mAb 735, in which there is a polysialic acid binding groove.[26] Previous ELISA-type assays have indicated that the DP preference of mAb 12E3 is for more than a 6-mer, and no limitations on the length.[12] The similarity in specificity and binding mode is compelling.

The structural flexibility of octyl-$(Neu5Ac)_3$ and $(Neu5Ac)_6$ might indicate that mAbs discriminate ligands accurately by selecting a minor conformer from a pre-existing equilibrium of structures,[36] rather than through an induced fit type mechanism.[37] Whatever the mechanism, it has been considered that the oligo- and polysialic acid antibodies discriminates their preferential DPs based on a conformational epitope. Our study shows that the bound conformation is different from the average original structure, and is stabilized as a consequence of binding. The mechanism of differential antigen recognition seems to arise from structural difference among the oligo/polysialic acids as well as the depth of the binding pocket/groove of the corresponding mAbs.

4. Conclusion

It is generally considered that the polysialic acid antibody discriminates a DP 10–15 from a shorter DP based on ligand structure and conformational epitope. We here provide an NMR-analysis directed at revealing the binding epitopes of anti-oligo/polysialic acid antibodies, A2B5 and 12E3. The mAb A2B5, whose preference is for DP3 rather than lesser or greater DPs, recognizes the sialic acid residues at the non-reducing terminus and nascent units. On the other hand, mAb 12E3, which prefers oligo/polysialic acids with DP>5, recognizes inner sialic acid residues. Interresidue transferred NOE correlations reveal that bound and free ligand structures are different in both cases. Such conformational alterations indicate that the free state of oligo sialic acids would be highly flexible having multi conformation[21,24] and the feasible binding mechanism is not of the key and lock type but rather a ligand-conformational proofreading model.

Our findings help to understand DP-dependent recognition of antibodies, and may be useful for the design of immunoreactive antigens to develop IgG-class anti-polysia antibodies and effective vaccines against polysia-containing bacteria.

Acknowledgements

We thank Dr. Y. Ito (RIKEN, ERATO) and Professor O. Kanie (ERATO, Tokai University) for use of the 500 MHz NMR facilities equipped with a cryo-TXI probe. We thank Ms. K. Matsumoto for the preparation of samples for NMR study and Ms. N. Tanaka for secretarial assistance.

Supplementary data

Supplementary data associated with this article can be found, in the online version, at http://dx.doi.org/10.1016/j.bmc.2013.07.023.

References and notes

1. Sato, C.; Kitajima, K. *Trends Glycosci. Glycotechnol.* **1999**, *11*, 371.
2. Nakata, D.; Troy, F. A. 2nd *J. Biol. Chem.* **2005**, *280*, 38305.
3. De Maria, R.; Lenti, L.; Malisan, F.; d'Agostino, F.; Tomassini, B.; Zeuner, A.; Rippo, M. R.; Testi, R. *Science* **1997**, *277*, 1652.
4. Hamamura, K.; Tsuji, M.; Hotta, H.; Ohkawa, Y.; Takahashi, M.; Shibuya, H.; Nakashima, H.; Yamauchi, Y.; Hashimoto, N.; Hattori, H.; Ueda, M.; Furukawa, K. *J. Biol. Chem.* **2011**, *286*, 18526.
5. Iber, H.; Zacharias, C.; Sandhoff, K. *Glycobiology* **1992**, *2*, 137.
6. Hirabayashi, Y.; Hirota, M.; Matsumoto, M.; Tanaka, H.; Obata, K.; Ando, S. *J. Biochem.* **1988**, *104*, 973.
7. Rutishauser, U.; Acheson, A.; Hall, A. K.; Mann, D. M.; Sunshine, J. *Science* **1988**, *240*, 53.
8. Rutishauser, U. *Nat. Rev. Neurosci.* **2008**, *9*, 26.
9. Ono, S.; Hane, M.; Kitajima, K.; Sato, C. *J. Biol. Chem.* **2012**, *287*, 3710.
10. Kanato, Y.; Kitajima, K.; Sato, C. *Glycobiology* **2008**, *18*, 104.
11. Troy, F. A. 2nd *Glycobiology* **1992**, *2*, 5.
12. Inoko, E.; Nishiura, Y.; Tanaka, H.; Takahashi, T.; Furukawa, K.; Kitajima, K.; Sato, C. *Glycobiology* **2010**, *20*, 916.
13. Sato, C.; Fukuoka, H.; Ohta, K.; Matsuda, T.; Koshino, R.; Kobayashi, K.; Troy, F. A.; Kitajima, K. *J. Biol. Chem.* **2000**, *275*, 15422.
14. Mackinnon, F. G.; Borrow, R.; Gorringe, A. R.; Fox, A. J.; Jones, D. M.; Robinson, A. *Microb. Pathog.* **1993**, *15*, 359.
15. Muhlenhoff, M.; Eckhardt, M.; Gerardy-Schahn, R. *Curr. Opin. Struct. Biol.* **1998**, *8*, 558.
16. Kahler, C. M.; Martin, L. E.; Shih, G. C.; Rahman, M. M.; Carlson, R. W.; Stephens, D. S. *Infect. Immun.* **1998**, *66*, 5939.
17. Frosch, M.; Gorgen, I.; Boulnois, G. J.; Timmis, K. N.; Bitter-Suermann, D. *Proc. Natl. Acad. Sci. U.S.A.* **1985**, *82*, 1194.
18. Sato, C.; Kitajima, K.; Inoue, S.; Seki, T.; Troy, F. A.; Inoue, Y. *J. Biol. Chem.* **1995**, *270*, 18923.
19. Jennings, H. J.; Roy, R.; Michon, F. *J. Immunol.* **1985**, *134*, 2651.
20. Battistel, M. D.; Shangold, M.; Trinh, L.; Shiloach, J.; Freedberg, D. I. *J. Am. Chem. Soc.* **2012**, *134*, 10717.
21. Yongye, A. B.; Gonzalez-Outeirino, J.; Glushka, J.; Schultheis, V.; Woods, R. J. *Biochemistry* **2008**, *47*, 12493.
22. Brisson, J. R.; Baumann, H.; Imberty, A.; Perez, S.; Jennings, H. J. *Biochemistry* **1992**, *31*, 4996.
23. Yamasaki, R.; Bacon, B. *Biochemistry* **1991**, *30*, 851.
24. Henderson, T. J.; Venable, R. M.; Egan, W. *J. Am. Chem. Soc.* **2003**, *125*, 2930.
25. Tchoghandjian, A.; Baeza, N.; Colin, C.; Cayre, M.; Metellus, P.; Beclin, C.; Ouafik, L.; Figarella-Branger, D. *Brain Pathol.* **2010**, *20*, 211.
26. Evans, S. V.; Sigurskjold, B. W.; Jennings, H. J.; Brisson, J. R.; To, R.; Tse, W. C.; Altman, E.; Frosch, M.; Weisgerber, C.; Kratzin, H. D., et al *Biochemistry* **1995**, *34*, 6737.
27. Johal, A. R.; Jarrell, H. C.; Letts, J. A.; Khieu, N. H.; Landry, R. C.; Jachymek, W.; Yang, Q.; Jennings, H. J.; Brisson, J. R.; Evans, S. V. *Glycobiology* **2013**, *23*, 946.
28. Mayer, M.; Meyer, B. *J.Am. Chem. Soc.* **2001**, *123*, 6108.
29. Mayer, M.; Meyer, B. *Angew. Chem., Int. Ed.* **1999**, *38*, 1784.
30. Glaudemans, C. P.; Lerner, L.; Daves, G. D., Jr.; Kovac, P.; Venable, R.; Bax, A. *Biochemistry* **1990**, *29*, 10906.
31. Post, C. B. *Curr. Opin. Struct. Biol.* **2003**, *13*, 581.
32. Bohm, R.; Freiberger, F.; Stummeyer, K.; Gerardy-Schahn, R.; von Itzstein, M.; Haselhorst, T. *Chembiochem* **2010**, *11*, 170.
33. Pichla, S. L.; Murali, R.; Burnett, R. M. *J. Struct. Biol.* **1997**, *119*, 6.
34. Saito, M.; Sugiyama, K. *Biochim. Biophys. Acta* **2000**, *1474*, 88.
35. Saito, M.; Kitamura, H.; Sugiyama, K. *J. Neurochem.* **2001**, *78*, 64.
36. Monod, J.; Wyman, J.; Changeux, J. P. *J. Mol. Biol.* **1965**, *12*, 88.
37. Koshland, D. E. *Proc. Natl. Acad. Sci. U.S.A.* **1958**, *44*, 98.